# Thermodynamics of Ion-Induced RNA Folding in the Hammerhead Ribozyme: An Isothermal Titration Calorimetric Study†

Christian Hammann,‡ Alan Cooper,§ and David M. J. Lilley*,‡

*CRC Nucleic Acid Structure Research Group, Department of Biochemistry, The University of Dundee, Dundee DD1 4HN, U.K., and Department of Chemistry, University of Glasgow, Glasgow G12 8QQ, U.K.*

*Received September 22, 2000; Revised Manuscript Received November 28, 2000*

ABSTRACT: The hammerhead ribozyme undergoes a well-defined two-stage conformational folding process, induced by the binding of magnesium ions. In this study, we have used isothermal titration calorimetry to analyze the thermodynamics of magnesium binding and magnesium ion-induced folding of the ribozyme. Binding to the natural sequence ribozyme is strongly exothermic and can be analyzed in terms of sequential interaction at two sites with association constants $K_A = 480$ and 2840 $M^{-1}$. Sequence variants of the hammerhead RNA give very different isothermal titration curves. An A14G variant that cannot undergo ion-induced folding exhibits endothermic binding. By contrast, a deoxyribose G5 variant that can undergo only the first of the two folding transitions gives a complex titration curve. However, despite these differences the ITC data for all three species can be analyzed in terms of the sequential binding of magnesium ions at two sites. While the binding affinities are all in the region of $10^3$ $M^{-1}$, corresponding to free energies of $\Delta G° = -3.5$ to $-4$ kcal $mol^{-1}$, the enthalpic and entropic contributions show much greater variation. The ITC experiments are in good agreement with earlier conformational studies of the folding of the ion-induced folding of the hammerhead ribozyme.

The biological function of RNA molecules is dependent upon folding into the correct three-dimensional structure. There is a very important electrostatic component in RNA structure, resulting from the charged phosphodiester backbone, and metal ions almost invariably play a critical role in stabilizing the folded structures. Catalytic RNA species provide especially useful systems for the study of ion-induced RNA structural transitions, because folding can be correlated with functional activity.

The hammerhead ribozyme (*1*−*3*) undergoes RNA-catalyzed site-specific cleavage, requiring only magnesium or similar cations for activity (*4*). It can be reduced to one or more pieces of RNA comprising about 50 nucleotides. The cleavage reaction occurs by a transesterification reaction, in which the 2′-oxygen atom attacks the 3′-phosphorus by an $S_N2$ mechanism. The products are 5′-hydroxyl and 2′,3′-cyclic phosphate termini (*5*, *6*), and the reaction proceeds with inversion of configuration at the phosphorus (*7*−*9*). Under normal circumstances one or more metal ions appear to play a direct role in the chemistry of cleavage. The reaction in the presence of magnesium ions is retarded by $R_p$ thiophosphate substitution (*9*) but can be restored in the presence of a softer ion such as manganese (*4*). However, this appears to be dispensable, since the ribozyme retains some activity in the presence of very high concentrations of lithium or even ammonium ions (*10*).

The hammerhead ribozyme comprises an elaborated three-way helical junction, where three helical sections are connected by the conserved core of formally single-stranded sections of 7, 3, and 1 nucleotide [a $HS_1HS_7HS_3$ junction (*11*)]. The position of self-cleavage is located within the shortest single-stranded section. The three-dimensional structure of the ribozyme has been determined by crystallography (*12*−*15*). Two main features contribute to the folded RNA structure observed in the crystal. The sequence C3U4G5A6 adopts the geometry of a turn found in the anticodon stem of tRNA and is termed domain 1; it is close to the scissile bond at C17 and is the probable catalytic core of the ribozyme. Domain 2 is formed by pairing between G12A13A14 and U7G8A9 and mediates coaxial alignment between helices II and III in the structure.

We have studied the ion-induced folding processes in the hammerhead ribozyme by comparative gel electrophoresis (*16*) and fluorescence resonance energy transfer (FRET)[1] (*17*). The structure adopted is dependent on both the type and concentration of metal ions present. In the absence of added ions the structure is extended, with no interhelical interactions. Upon addition of metal ions, folding occurs in two distinct steps (Figure 1). In the presence of 500 $\mu$M magnesium ions the hammerhead adopts a structure in which there is a large angle between helices II and III, and it is likely that this stage corresponds to the formation of domain 2. As the magnesium ion concentration is increased over the range of 1−15 mM magnesium ions, there is a further folding in which helix I changes position from being directed in a

† This work was financially supported by the CRC, EPSRC, and BBSRC.

* To whom correspondence should be addressed. Tel: (44)-1382-344243. Fax: (44)-1382-201063. E-mail: dmjlilley@bad.dundee.ac.uk.

‡ The University of Dundee.

§ University of Glasgow.

[1] Abbreviations: ITC, isothermal titration calorimetry; FRET, fluorescence resonance energy transfer.

10.1021/bi002231o CCC: $20.00 
Published on Web 01/09/2001

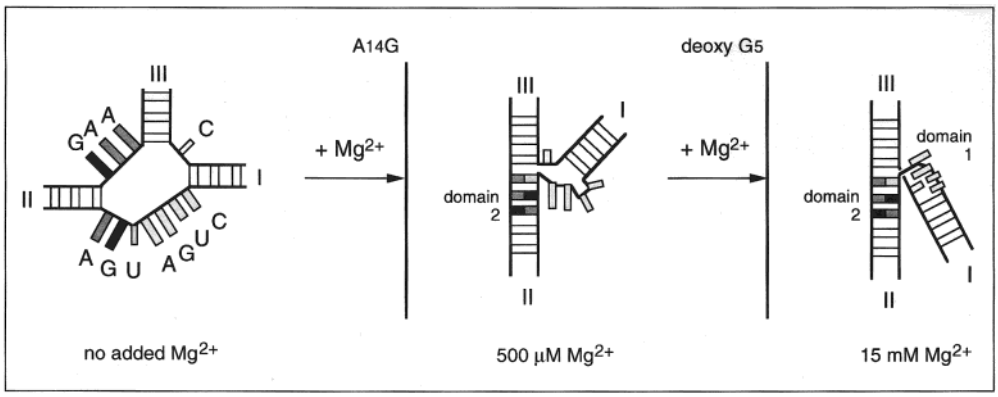


FIGURE 1: Two-stage ion-induced folding of the hammerhead ribozyme. The schematic illustrates the folding scheme deduced from comparative gel electrophoresis and FRET studies. The first stage occurs in the 0−500 $\mu$M range of magnesium ion concentration and results in the formation of domain 2 by coaxial interaction between stems II and III. This folding event is blocked in the A14G sequence variant. Domain I, the catalytic core of the ribozyme, is formed in the second transition occurring in the 1−15 mM range of magnesium ion concentration. This occurs by the formation of a uridine turn by the sequence C3U4G5A6, resulting in a repositioning of stem I in the same quadrant as stem II. Removal of the 2′-hydroxyl group of G5 (or the change G5C) blocks the second transition.

similar direction to helix III to being close to helix II. This magnesium ion concentration range corresponds closely to that for catalytic activity (*4*), and this transition most probably reflects the formation of domain 1, the catalytic core of the ribozyme. The global structure of the RNA under these conditions is in good agreement with the structure seen in the crystal structures (*12*, *13*) and in an earlier FRET study (*18*). More detailed analysis of the ion dependence of the folding suggests that both transitions are simple two-state processes with Hill coefficients of unity (*17*). The simplest model for the overall folding process that is consistent with these data would be a two-step process, each of which is induced by the binding of a single metal ion.

The characterization of sequence variants that exhibit perturbed ion-induced folding is consistent with this scheme (*19*, *20*). The second stage of folding (i.e., the proposed formation of domain 1) is blocked by changes at G5; however, the first stage of folding is essentially unaffected by changes at G5. Changes in the sequences that participate in domain 2 lead to more radical alterations in folding. Thus the base changes A14G and G8U lead to an apparent total blockage of all tertiary folding, while A13G leads to folding into an aberrant misfolded form (*20*). These variants provide a useful resource for additional studies.

To date little has been learned concerning the thermodynamics of the folding of the hammerhead ribozyme. Since the folding process is induced by the addition of magnesium ions, we have employed isothermal titration calorimetry (ITC) to analyze the energetics, using the folding variants to dissect the different stages. We find that the natural hammerhead sequence folds in an exothermic process that can be analyzed in terms of two sequential ion binding events.

## MATERIALS AND METHODS

*Chemical Synthesis of RNA-Containing Oligonucleotides.* Oligonucleotides containing both DNA and RNA sections were synthesized using phosphoramidite chemistry implemented on Applied Biosystems 394 DNA/RNA synthesizers. RNA sections were synthesized using ribonucleotide phosphoramidites with 2′-*tert*-butyldimethylsilyl protection (Pro-Oligo). Three 200 nmol scale syntheses of each hammerhead derivative were required for the ITC experiments. Oligoribonucleotides were deprotected and purified as described previously (*17*).

*Design of Hammerhead Ribozyme Species for ITC Measurements*. The following 59 nt sequences were synthesized: natural sequence hammerhead ribozyme, 5′ CCGTGAGCGUCUGAGCGTAAGCUCACUGAUGAGGCCCGTAAGGGCCGAAACGCTCACGG 3′; A14G variant sequence, 5′CCGTGAGCGUCUGAGCGTAAGCUCACUGAUGAGGCCCGTAAGGGCCGAGACGCTCACGG 3′; deoxy-G5 variant, 5′ CCGTGAGCGUCUGAGCGTAAGCUCACUGAUGAGGCCCGTAAGGGCCGAAACGCTCACGG 3′. Underlined bases indicate deoxyribose substitutions. All versions of the hammerhead contained deoxyribose substitutions at C17 to prevent self-cleavage occurring in the presence of magnesium ions. Helix III was extended to 10 base pairs in order to ensure efficient formation of the secondary structure.

*Calorimetry*. ITC measurements were carried out at 10 or 25 °C using a VP-ITC titration calorimeter (MicroCal, Northampton, MA). All solutions were degassed before titrations. RNA solutions were extensively dialyzed against the same buffer containing 50 mM Tris·HCl (pH 8.0) and 100 mM NaCl. The high background concentration of monovalent cations was used to reduce nonspecific electrostatic interaction with the charged RNA backbone and to reduce heat effects due to dilution of magnesium ions. Magnesium chloride solution was prepared by dissolving the salt in dialysis buffer. Titration was carried out using a 370 $\mu$L syringe, with stirring at 400 rpm. Each titration consisted of a preliminary 1 $\mu$L injection, followed by 20−30 subsequent injections of various increasing volumes (4 × 3 $\mu$L, 6 × 5 $\mu$L, 6 × 10 $\mu$L, 14 × 15 $\mu$L) into a cell containing approximately 1.4 mL of a 65 $\mu$M RNA solution. This procedure was chosen to cover a wide magnesium ion concentration range from 50 $\mu$M to 5 mM). Calorimetric data were analyzed using MicroCal ORIGIN software. To correct for dilution and mixing effects, a series of control injections was carried out, in which magnesium chloride was injected in buffer alone. The heat signal of this control was then subsequently subtracted from the raw data for each RNA species.

## RESULTS

*Analysis of the RNA−Magnesium Association and Magnesium-Induced Folding of the Hammerhead Ribozyme Using Isothermal Titration Microcalorimetry*. We have used isothermal titration calorimetry (ITC) (*21*) to determine directly the energetics and stoichiometry of the interaction between the hammerhead ribozyme (or folding variants) and magnesium ions. In these experiments, aliquots of a magnesium chloride solution are injected into a concentrated RNA solution contained in the calorimeter sample cell, and the heat energy changes accompanying the RNA−$Mg^{2+}$ association and the induced RNA folding processes are detected upon each injection. Detailed descriptions of the background to this method can be found in Ladbury and Chowdhry (*22*). Experiments are carried out in a titration calorimeter that houses a sample and a reference cell in a thermally insulated jacket, which is set to the desired experimental temperature with an accuracy of $10^{-4}$ °C. Absorption or evolution of heat energy upon injection of magnesium is measured as the power ($dq/dt$, $\mu$cal $s^{-1}$) that is required to maintain zero temperature difference between the sample and the reference cell. The raw data obtained this way are corrected for dilution effects by subtracting heat energy changes per unit time measured in an identical series of titrations of magnesium into buffer. Integration of the resulting data over time allows the determination of the heat $\Delta Q(i)$ (kcal/mol of injected magnesium) that had to be added or removed to restore the thermal equilibrium between sample and reference cells after the $i$th injection of magnesium to the RNA. This series of $\Delta Q(i)$ values is plotted against magnesium ion concentration, representing the differential of the total heat $Q$ [i.e., enthalpy ($\Delta H$) at constant pressure] for each magnesium concentration. Individual heat energy changes $\Delta Q(i)$ thus are related in a simple bimolecular interaction (here as $n$ $Mg^{2+}$ ions interact with one type of binding site in the RNA) by

$$\Delta Q(i) = nfc_{\mathrm{RNA}}\Delta HV \tag{1}$$

with fractional saturation $f$, total RNA concentration $c_{\mathrm{RNA}}$, and calorimetry cell volume $V$. The total RNA concentration is related to the free RNA concentration and the total magnesium ion concentration $c_{\mathrm{Mg}}$ through the association constant $K_{\mathrm{A}}$ and thus

$$\Delta Q(i) = nc_{\mathrm{RNA}}\Delta H\frac{V}{2}\left[1 + \frac{c_{\mathrm{Mg}}}{nc_{\mathrm{RNA}}} + \frac{1}{nK_{\mathrm{A}}c_{\mathrm{RNA}}} - \sqrt{\left(1 + \frac{c_{\mathrm{Mg}}}{nc_{\mathrm{RNA}}} + \frac{1}{nK_{\mathrm{A}}c_{\mathrm{RNA}}}\right)^2 - \frac{4c_{\mathrm{Mg}}}{nc_{\mathrm{RNA}}}}\right] \tag{2}$$

This equation shows that $\Delta Q(i)$ is dependent on the values of the independent parameters $\Delta H$, $K_{\mathrm{A}}$, and $n$, which can be determined by fitting binding simulations for $\Delta Q(i)$ throughout the titration (*22*). Knowing the association constant ($K_{\mathrm{A}}$) and enthalpy change ($\Delta H°$) for each type of binding site permits the calculation of changes in standard Gibbs free energy ($\Delta G°$) and entropy ($\Delta S°$). In addition, changes in molar heat capacity ($\Delta C_p$) can be obtained from measurements at different temperatures.

For these experiments we synthesized a cloverleaf-form hammerhead ribozyme, formed from a single strand (Figure 2). The core of this species comprises RNA except for deoxyribose substitution at C17 to prevent self-cleavage. The helical arms contain RNA for the interior 3 bp and DNA elsewhere to maximize the efficiency of synthesis; these positions do not affect ribozyme folding. To dissect the influence of magnesium ions on each of the two stages of the folding process, variant ribozymes A14G and dG5 were synthesized (see Figure 2). These variants are totally blocked (A14G) or blocked after the first folding stage (dG5) (*19*, *20*), as discussed above.

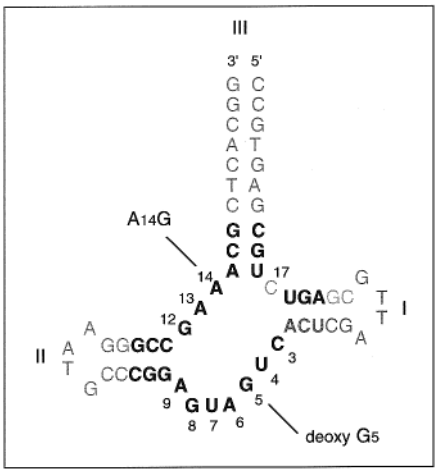


FIGURE 2: Sequence of the cloverleaf hammerhead construct used for calorimetric measurements. The molecule comprises a single strand forming helix III of 10 bp and helices I and III, each of which comprise 5 bp closed by a tetraloop. DNA residues are shown in gray, and RNA residues are shown in bold letters. The numbering system follows Hertel et al. (*26*). Nucleotide variations have been introduced as indicated.

*The Natural Sequence Hammerhead Ribozyme*. Titration of the natural sequence hammerhead ribozyme with magnesium ions revealed exothermic binding properties (Figure 3, upper panel). Discontinuities in the heat pulse profile correspond to programmed changes in injection volume. After correction for a dilution control, the integrated heat data were plotted against the molar ratio of magnesium ions to RNA (Figure 3, lower panel). In this presentation, the heat evolved per injection decreases with increasing magnesium ion concentrations. Initial magnesium ion injections give rise to an exothermic (negative) heat response, decreasing with subsequent injections to become slightly endothermic (positive) before approaching zero asymptotically at high magnesium ion concentrations. Such behavior is inconsistent with a single metal ion binding model. We therefore fitted the data to a model in which two ions bind sequentially, according to

$$\mathrm{RNA} \underset{K_1}{\overset{\mathrm{Mg}}{\rightleftharpoons}} \mathrm{RNA{\cdot}Mg} \underset{K_2}{\overset{\mathrm{Mg}}{\rightleftharpoons}} \mathrm{RNA{\cdot}Mg_2}$$

$$K_1 = \frac{[\mathrm{RNAMg}]}{[\mathrm{RNA}][\mathrm{Mg}]}$$

$$K_2 = \frac{[\mathrm{RNA(Mg)_2}]}{[\mathrm{RNAMg}][\mathrm{Mg}]} \tag{3}$$

$$Q = [\mathrm{RNA}]_t V_o \frac{K_1[\mathrm{Mg}]\Delta H_1 + K_1K_2[\mathrm{Mg}]^2(\Delta H_1 + \Delta H_2)}{1 + K_1[\mathrm{Mg}] + K_1K_2[\mathrm{Mg}]^2} \tag{4}$$

where $K_1$ and $K_2$ are the binding constants, $Q$ is the total

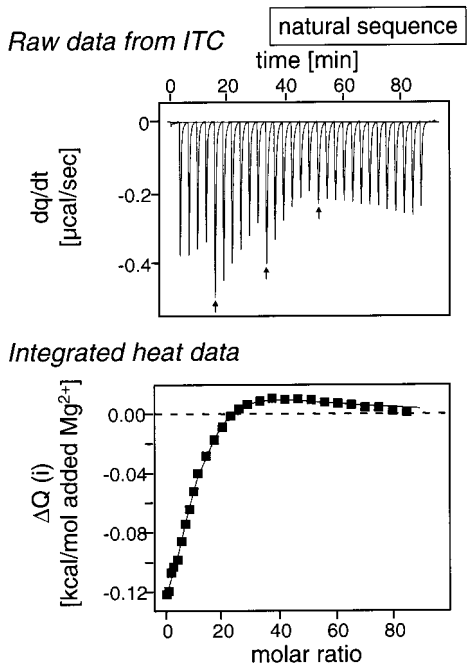


FIGURE 3: Isothermal titration calorimetry of the interaction of magnesium ions with the natural sequence hammerhead ribozyme. Magnesium chloride was titrated into a 65 $\mu$M RNA solution, and the heat evolved was monitored by ITC. Upper panel: Raw data for sequential injection of various volumes (3, 5, 10, or 15 $\mu$L) of a 35 mM magnesium chloride solution into 1.4 mL of RNA solution in 50 mM Tris·HCl (pH 8.0) and 100 mM NaCl at 283 K. The apparent discontinuities in the heat profile are due to changes in injection volumes at the positions indicated by arrows. Lower panel: Integrated heat data, corrected for exothermic magnesium ion dilutions, were fitted according to a sequential two-ion binding model (continuous line). The thermodynamic parameters for the two sequential binding events are summarized in Table 1.

heat content, $V_o$ is the active cell volume, [Mg] is the free magnesium ion concentration, and $[RNA]_t$ is the total RNA concentration.

This was the simplest model that gave a good fit to the experimental data, shown in the lower panel of Figure 3. A model assuming two independent ion binding events gave a considerably poorer fit and exhibited a higher $\chi^2$ value (data not shown). The thermodynamic parameters obtained by the application of the sequential binding model are summarized in Table 1. We observe an initial binding event with an association constant of 480 $\pm$ 90 $M^{-1}$, which is largely dominated by the enthalpy contribution. The second binding event is stronger with an apparent association constant of 2840 $\pm$ 650 $M^{-1}$, indicating cooperativity. It is dominated by the change in entropy, with a positive enthalpy contribution.

A second titration with magnesium, carried out at 298 K, allowed an estimation of the heat capacity ($\Delta C_p$) of this binding event. For this purpose, volumes of 5 and 10 $\mu$L of a 10 mM magnesium chloride solution were injected in 1.4 mL of a 17 $\mu$M RNA solution at a temperature of 298 K, covering a magnesium ion concentration range between 35 $\mu$M and 2 mM. The overall shape of the thermal titration curve was nearly identical to that observed at the lower temperature of 283 K; however, a weaker signal was detected, due to the lower concentration of RNA used (data not shown). The raw data were corrected by a dilution control (at 298 K), and the integrated heat data were fitted to the two-ion sequential binding model (data not shown). A comparison of $\Delta H°_{298}$ and $\Delta H°_{283}$ revealed that the heat capacity change for both binding events is very small (Table 1).

The two-ion sequential model provides an acceptable fit for the calorimetry data, and two sequential metal ions have also been observed (but not the cooperative behavior) by the analysis of ion-induced folding using FRET (*17*). However, we wanted to examine the possibility that the very high RNA concentration (65 $\mu$M) used in this study led to intermolecular RNA−RNA interactions, such as dimerization, which we had observed previously in cloverleaf hammerhead ribozymes at a concentration of about 200 $\mu$M (data not shown). For this purpose, we repeated the ITC experiments at 283 K, using a reduced RNA concentration of 35 $\mu$M. The shape of the titration curve observed using this lower concentration was virtually identical to that at 65 $\mu$M. The strength of the signal, however, was reduced due to the lower RNA concentration (data not shown). Furthermore, the results obtained from the titration of a 17 $\mu$M RNA solution at 298 K (see above) confirm that the heat signal we observe is due to the interaction of magnesium ions with individual RNA molecules.

*The A14G Variant Hammerhead Ribozyme*. The evolution of heat observed on titration of the hammerhead ribozyme with magnesium ions is expected to be the algebraic sum of two enthalpic components. The first is that due to the binding of the ion to the RNA, and the second arose from changes in the conformation of the RNA induced on binding. We have used previously characterized folding variants to try to differentiate between these components. Using comparative gel electrophoresis and FRET, we have shown that the variant A14G is unable to fold into either the intermediate or final forms of the ribozyme and remains in an extended conformation (probably with helix III extended by 1 or 2 base pairs) (*19*).

Isothermal titration of the A14G hammerhead ribozyme with magnesium ions was strongly endothermic (Figure 4, upper panel), in complete contrast to the wild-type sequence. Clearly, the radically different folding property of this sequence is reflected in its thermal behavior.

It is apparent from the integrated heat data in the lower panel of Figure 4 that the interaction of magnesium ions with the A14G variant is composed of two separate events, and we therefore used the same two-ion sequential binding model to fit the data. The thermodynamic parameters are presented in Table 1. Here, the initial binding event corresponds to an association constant of 1230 $\pm$ 320 $M^{-1}$. The binding is largely driven by the change in entropy, with a very small contribution of enthalpy toward $\Delta G°$. The small (probably not significant) negative heat capacity $\Delta C_p = -0.02 \pm 0.01$ kcal $mol^{-1}$ $K^{-1}$ was determined from the enthalpy contributions at 283 and 298 K.

The association constant for the second binding event is virtually identical to that observed for the first binding event of the wild-type ribozyme. Thus, metal binding in the A14G variant does not proceed cooperatively. The main contribution to the free energy of the second binding event is the entropy change, and a significant negative change in heat capacity $\Delta C_p = -0.34 \pm 0.02$ kcal $mol^{-1}$ $K^{-1}$ was obtained.

Isothermal titrations were carried out at RNA concentrations of 35 $\mu$M ($T$ = 283 K) and 17 $\mu$M ($T$ = 298 K) to test

Table 1: Thermodynamic Parameters at 283 K Calculated for the Hammerhead Ribozyme and Derivatives by Application of the Two-Ion Sequential Binding Model

| RNA | binding site | $K_A$ ($\times 10^3$ $M^{-1}$) | $\Delta G°$ (kcal $mol^{-1}$) | $\Delta H°$ (kcal $mol^{-1}$) | $\Delta S°$ (cal $mol^{-1}$ $K^{-1}$) | $\Delta C_p$ (kcal $mol^{-1}$ $K^{-1}$) |
|---|---|---|---|---|---|---|
| natural | 1 | $0.5 \pm 0.1$ | $-3.5 \pm 0.1$ | $-4.3 \pm 0.7$ | $(-2.8 \pm 2.2)^a$ | $(-0.001 \pm 0.02)^a$ |
| | 2 | $2.8 \pm 0.7$ | $-4.5 \pm 0.1$ | $3.1 \pm 0.8$ | $27 \pm 3$ | $(0.01 \pm 0.04)^a$ |
| A14G | 1 | $1.2 \pm 0.3$ | $-4.0 \pm 0.2$ | $0.3 \pm 0.1$ | $15 \pm 1$ | $-0.02 \pm 0.01$ |
| | 2 | $0.5 \pm 0.1$ | $-3.5 \pm 0.1$ | $5.7 \pm 0.4$ | $33 \pm 2$ | $-0.34 \pm 0.02$ |
| dG5 | 1 | $0.4 \pm 0.1$ | $-3.3 \pm 0.1$ | $-0.1 \pm 0.1$ | $11 \pm 1$ | $-0.67 \pm 0.04$ |
| | 2 | $1.1 \pm 0.2$ | $-3.9 \pm 0.1$ | $2.5 \pm 0.1$ | $23 \pm 1$ | $0.78 \pm 0.04$ |

[a] This value is insignificant, since the error is comparable with the measurement.

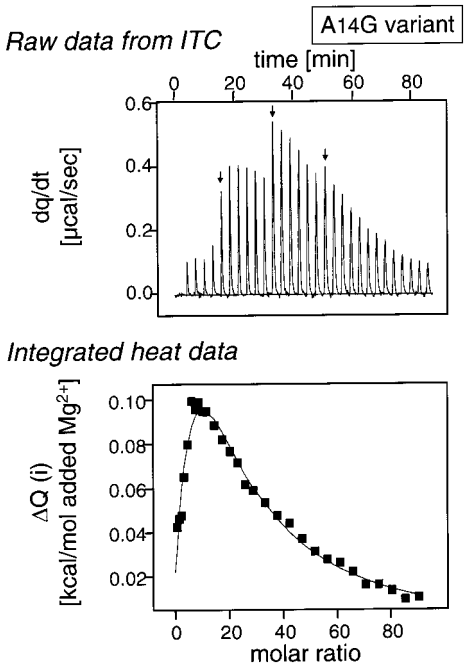


FIGURE 4: Isothermal titration calorimetry of the interaction of magnesium ions with the hammerhead ribozyme variant A14G. Magnesium chloride was titrated into a 65 $\mu$M RNA solution, and the heat absorbed was monitored by ITC. Upper panel: Raw data for the sequential injection of various volumes (3, 5, 10, or 15 $\mu$L) of a 35 mM magnesium chloride solution into 1.4 mL of RNA solution in 50 mM Tris·HCl (pH 8.0) and 100 mM NaCl at 283 K. The apparent discontinuities in the heat profile are due to changes in injection volumes at the positions indicated by arrows. Lower panel: Integrated heat data (dilution corrected) with a fit according to a sequential two-ion binding model (continuous line). The derived thermodynamic parameters are summarized in Table 1.

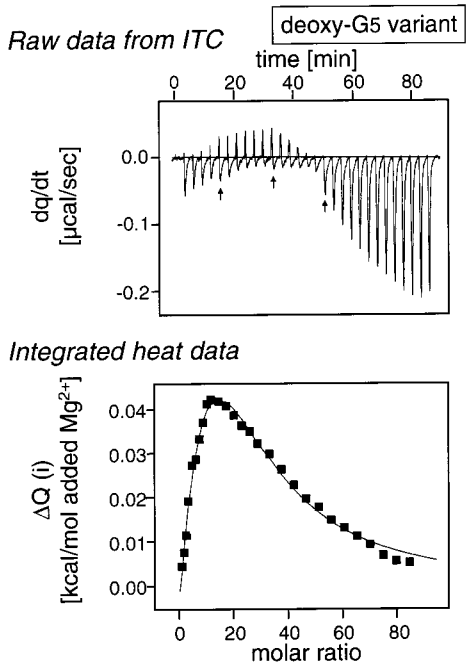


FIGURE 5: Isothermal titration calorimetry of the interaction of magnesium ions with the deoxy-G5 hammerhead ribozyme. Magnesium chloride was titrated into a 65 $\mu$M RNA solution, and the complex heat changes were monitored by ITC. Upper panel: Raw data for the sequential injection of various volumes (3, 5, 10, or 15 $\mu$L) of a 35 mM magnesium chloride solution into 1.4 mL of RNA solution in 50 mM Tris·HCl (pH 8.0) and 100 mM NaCl at 283 K. Due to changes in the injection volumes (at the positions indicated by arrows), the raw data do not appear as a continuously varying heat change. Lower panel: Integrated heat data (dilution corrected) with a fit according to a sequential two-ion binding model (continuous line). The derived thermodynamic parameters are summarized in Table 1.

for the possibility of RNA−RNA association. As in the case of the wild-type ribozyme, only the strength of the signal was reduced and the shape of the biphasic heat curve remained virtually unchanged, indicating specific interaction between magnesium ions and individual RNA molecules.

*Deoxy-G5-Modified Hammerhead Ribozyme*. Removal of the 2′-hydroxyl group from G5 in the CUGA sequence that forms the domain 1 structure in the natural sequence ribozyme leads to an intermediate form of folding. According to analysis by comparative gel electrophoresis (*19*) and FRET (*20*), this sequence undergoes the first stage of folding but is unable to form domain 1.

Isothermal titration calorimetry of magnesium ion binding to the deoxy-G5 form of the ribozyme shows a qualitatively similar pattern to that of the A14G variant (Figure 5, upper panel). Binding is initially athermal ($\Delta H° \approx 0$) but becomes progressively more endothermic before falling back to baseline as (presumably) all magnesium ion sites become saturated at higher concentrations. Additionally, the individual heat changes on ion additions are kinetically complex; the intermediate, endothermic signals (injections 4−11) comprise a kinetically faster endothermic part, followed by a kinetically slower exothermic part. These data again show how the altered folding properties of the modified ribozyme are reflected in very different thermal properties compared to the natural form of the RNA.

After correction for dilution effects, the overall integrated heat data were endothermic, as shown in the lower panel of Figure 5. From this, it is apparent that the interaction of magnesium ions with the deoxy-G5 hammerhead RNA is composed of two different events. As before, the data were fitted to a sequential two-ion binding model. The thermodynamic parameters are presented in Table 1. As with the wild-type ribozyme (but not the A14G variant), a slightly

cooperative magnesium ion binding is observed with the weaker binding occurring first. This event exhibits an association constant of 360 ± 80 $M^{-1}$, which is slightly reduced relative to the wild type. The event is driven by the change in entropy, with a negligible contribution of enthalpy. However, the data obtained at 298 K revealed a rather large negative heat capacity of $\Delta C_p = -0.67 \pm 0.04$ kcal $mol^{-1}$ $K^{-1}$.

The strong binding is characterized by an association constant of 1060 ± 200 $M^{-1}$, equivalent within the experimental error to the strong binding observed for the A14G variant and lower than that of the natural sequence. As with the natural ribozyme, the binding is driven by the entropy change, with a positive enthalpy contribution. In contrast to the natural sequence RNA, however, a large positive heat capacity $\Delta C_p = 0.776 \pm 0.037$ kcal $mol^{-1}$ $K^{-1}$ was determined by comparison of the enthalpies determined at 283 and 298 K. ITC experiments employing lower RNA concentrations of 35 $\mu$M at 283 K or 17 $\mu$M at 298 K indicated that RNA−RNA interactions were unimportant (data not shown).

## DISCUSSION

We have shown that the energetics of magnesium ion binding to the hammerhead ribozyme can be studied using isothermal titration calorimetry. The most striking result from these experiments is the great difference in isothermal titration curves between the three hammerhead RNAs (Figures 3−5). However, despite these differences, the ITC experiments show that binding of magnesium ions to each of these hammerhead ribozymes follows a similar pattern involving sequential binding to two sites, with binding affinities (association constant $K_A$) in the region of 1000 $M^{-1}$, corresponding to standard Gibbs free energies ($\Delta G°$) in the region of −3.5 to −4 kcal/mol. The enthalpic and entropic contributions that make up this free energy show much greater variation, both within and between variants, with metal ion binding to the second site being consistently more endothermic than to the first. As is commonly observed in macromolecular interactions (*23*), these $\Delta H°$ and $\Delta S°$ variations tend to compensate to give much smaller differences in binding free energy.

The sequential two-ion binding model used to fit the calorimetric data for the natural sequence hammerhead ribozyme is consistent with our earlier studies by comparative gel electrophoresis and FRET. These studies were interpreted in terms of a two-stage folding process (summarized in Figure 1). Using two-state models for these transitions, we were able to estimate apparent magnesium ion association constants of approximately $K_A = 10\,000$ $M^{-1}$ for the first and 1000 $M^{-1}$ for the second binding event. From the calorimetric titrations we have calculated values of $K_A =$ 2840 and 480 $M^{-1}$ for the two transitions. The values we observe here are thus reduced approximately 2−3-fold, which is likely to be caused by the higher background concentration of monovalent metal ions present during the ITC experiments.

Closer inspection of the thermodynamic parameters suggests some correlation with conformational changes inferred from data obtained by other techniques. While both the A14G and deoxy-G5 variants give data that can be interpreted in terms of the sequential two-ion binding model, the calculated thermodynamic properties are mostly very different, as would be expected from the markedly different titration properties of these species. The exception is the higher affinity binding event of the deoxy-G5 variant hammerhead, which has values of $\Delta H°$, $K_A$, $\Delta G°$, and $\Delta S°$ similar to those of the higher affinity binding observed in the natural ribozyme sequence. This is in agreement with our proposal (*19*, *20*) that the removal of the 2′-hydroxyl from G5 allows the ribozyme to undergo the first folding transition (formation of domain 2) but prevents progression to the final folded state in which domain 1 is correctly folded. In the absence of magnesium ion-induced conformational changes (A14G), the binding free energies at the two sets of sites are very similar, although the enthalpies and entropy changes differ. For the natural system, binding to the first site is slightly weaker though more exothermic, consistent with a picture involving a ligand-induced conformational change using up some of the binding free energy to collapse the ribozyme into a conformational state with greater affinity for binding to the second site. The deoxy-G5 variant exhibits intermediate behavior in line with only partial capacity for conformational rearrangements.

A manganese ion has been observed bound to P9 in the hammerhead ribozyme crystal (*14*), and $R_p$ phosphorothioate substitution at this position leads to loss of catalytic activity (*24*). This would be a strong candidate for the ion that is responsible for the first folding transition, and $R_p$ phosphorothioate substitution at P9 leads to poor folding in magnesium ions (G. S. Bassi and D. M. J. Lilley, unpublished data). The second transition may be induced by ion binding at P6. Terbium(III) ions have been observed bound in this region by crystallography (*25*), $S_p$ phosphorothioate substitution at this position leads to loss of catalytic activity, and uranyl ions have been located by photocleavage in the vicinity of G5 (*16*). The uranyl photocleavage site is only detected late in the folding process (*20*).

In summary, the ITC experiments give good agreement with earlier studies of the folding of the ion-induced folding of the hammerhead ribozyme and reveal the major conformational effect of the A14G and deoxy-G5 sequence variants. These studies show that ITC is a powerful approach for the study of ion-induced folding in RNA, and we anticipate a more general application in the future.

## ACKNOWLEDGMENT

We thank Drs. Sonya Melcher, Z. Zhao, Tim Wilson, and Dan Lafontaine for valuable discussion and Margaret Nutley for technical assistance.

## REFERENCES

1. Forster, A. C., and Symons, R. H. (1987) *Cell 49*, 211−220.
2. Hazeloff, J. P., and Gerlach, W. L. (1988) *Nature 334*, 585−591.
3. Epstein, L. M., and Gall, J. G. (1987) *Cell 48*, 535−543.
4. Dahm, S. C., and Uhlenbeck, O. C. (1991) *Biochemistry 30*, 9464−9469.
5. Hutchins, C. J., Rathjen, P. D., Forster, A. C., and Symons, R. H. (1986) *Nucleic Acids Res. 14*, 3627−3640.
6. Uhlenbeck, U. C. (1987) *Nature 328*, 596−600.
7. van Tol, H., Buzayan, J. M., Feldstein, P. A., Eckstein, F., and Bruening, G. (1990) *Nucleic Acids Res. 18*, 1971−1975.

8. Koizumi, M., and Ohtsuka, E. (1991) *Biochemistry 30*, 5145−5150.
9. Slim, G., and Gait, M. J. (1991) *Nucleic Acids Res. 19*, 1183−1188.
10. Murray, J. B., Seyhan, A. A., Walter, N. G., Burke, J. M., and Scott, W. G. (1998) *Chem. Biol. 5*, 587−595.
11. Lilley, D. M. J., Clegg, R. M., Diekmann, S., Seeman, N. C., von Kitzing, E., and Hagerman, P. (1995) *Eur. J. Biochem. 230*, 1−2.
12. Pley, H. W., Flaherty, K. M., and McKay, D. B. (1994) *Nature 372*, 68−74.
13. Scott, W. G., Finch, J. T., and Klug, A. (1995) *Cell 81*, 991−1002.
14. Scott, W. G., Murray, J. B., Arnold, J. R. P., Stoddard, B. L., and Klug, A. (1996) *Science 274*, 2065−2069.
15. Murray, J. B., Terwey, D. P., Maloney, L., Karpeisky, A., Usman, N., Beigelman, L., and Scott, W. G. (1998) *Cell 92*, 665−673.
16. Bassi, G., Møllegaard, N. E., Murchie, A. I. H., von Kitzing, E., and Lilley, D. M. J. (1995) *Nat. Struct. Biol. 2*, 45−55.
17. Bassi, G. S., Murchie, A. I. H., Walter, F., Clegg, R. M., and Lilley, D. M. J. (1997) *EMBO J. 16*, 7481−7489.
18. Tuschl, T., Gohlke, C., Jovin, T. M., Westhof, E., and Eckstein, F. (1994) *Science 266*, 785−789.
19. Bassi, G. S., Murchie, A. I. H., and Lilley, D. M. J. (1996) *RNA 2*, 756−768.
20. Bassi, G. S., Møllegaard, N. E., Murchie, A. I. H., and Lilley, D. M. J. (1999) *Biochemistry 38*, 3345−3354.
21. Wiseman, T., Williston, S., Brandts, J. F., and Lin, L. N. (1989) *Anal. Biochem. 179*, 131−137.
22. Ladbury, J. E., and Chowdhry, B. Z. (1996) *Chem. Biol. 3*, 791−801.
23. Cooper, A. (1999) *Curr. Opin. Chem. Biol. 3*, 557−563.
24. Ruffner, D. E., and Uhlenbeck, O. C. (1990) *Nucleic Acids Res. 18*, 6025−6029.
25. Feig, A. L., Scott, W. G., and Uhlenbeck, O. C. (1998) *Science 279*, 81−84.
26. Hertel, K. J., Pardi, A., Uhlenbeck, O. C., Koizumi, M., Ohtsuka, E., Uesugi, S., Cedergren, R., Eckstein, F., Gerlach, W. L., Hodgson, R., and Symons, R. H. (1992) *Nucleic Acids Res. 20*, 3252.

BI002231O